

Comparison of seasonal surface temperature trend, spatial variability, and elevation dependency from satellite-derived products and numerical simulations over the Tibetan Plateau from 2003 to 2011

Xiaoying Ouyang, Dongmei Chen, Yao Feng & Yonghui Lei

To cite this article: Xiaoying Ouyang, Dongmei Chen, Yao Feng & Yonghui Lei (2018): Comparison of seasonal surface temperature trend, spatial variability, and elevation dependency from satellite-derived products and numerical simulations over the Tibetan Plateau from 2003 to 2011, International Journal of Remote Sensing, DOI: [10.1080/01431161.2018.1482024](https://doi.org/10.1080/01431161.2018.1482024)

To link to this article: <https://doi.org/10.1080/01431161.2018.1482024>



Published online: 20 Jun 2018.



Submit your article to this journal [↗](#)



Article views: 4



View related articles [↗](#)



View Crossmark data [↗](#)



Comparison of seasonal surface temperature trend, spatial variability, and elevation dependency from satellite-derived products and numerical simulations over the Tibetan Plateau from 2003 to 2011

Xiaoying Ouyang ^{a,b}, Dongmei Chen ^b, Yao Feng^b and Yonghui Lei^a

^aState Key Laboratory of Remote Sensing Science, Institute of Remote Sensing and Digital Earth, Chinese Academy of Sciences, Beijing, China; ^bDepartment of Geography and Planning, Queen's University, Kingston, ON, Canada

ABSTRACT

Land surface temperature (LST) and near-surface air temperature products have been commonly used in the studies of global climate change. In this work, we compare satellite-observed LST from Advanced Along-Track Scanning Radiometer (AATSR) and surface skin temperature and 2 m air temperature (T2) simulated from High Asian Refined analysis (HAR) to provide an independent overview of the surface/air temperature trend over Tibetan Plateau (TP) region in 2003–2011. We investigate the seasonal trend, spatial variability, and the elevation dependency of LST and air temperature over TP for the last decade. Linear regression method is applied to all data sets to illustrate the warming and cooling trends and variability of temperature over the study area. Our analysis shows that an overall warming slope is 0.04 K year^{-1} in the day trend and 0.05 K year^{-1} in the night and the trend slope is stronger in the simulated HAR data sets than that in the AATSR LST, especially for the night air temperature. However, in regions with elevation above 4000 m, the proportion of areas with the warming trend is less than 50% except in autumn from HAR data sets. The Namco and Qomolangma sites show an apparent trend of warming and cooling, respectively. The results from both satellite observations and numerical outputs show that warming trend over the entire TP was not obvious during last decade and the cooling trend was even found in the northeast TP.

ARTICLE HISTORY

Received 1 December 2017

Accepted 15 May 2018

1. Introduction

Tibetan Plateau (TP) is one of the most sensitive areas to global warming (Liu and Chen 2000). Research regarding the warming trend over TP is one of the main challenges in regional and global climate studies due to sparsely distributed ground stations, particularly in the western TP where elevation is over 4800 m (Qin et al. 2009). Meanwhile, thermal remote-sensing satellite observations and numerical simulations provide broad spatial coverage of the land surface temperature (LST) independently (Li et al. 2013; Duan et al. 2014a; Duan, Li, and Leng

CONTACT Dongmei Chen chendm@queensu.ca Department of Geography and Planning, Queen's University, Kingston, ON K7L 3N6, Canada

© 2018 Informa UK Limited, trading as Taylor & Francis Group

2017; Qin, Karnieli, and Berliner 2001b; Qin et al. 2001a; Cheng et al. 2010). Additionally, the elevation dependency of temperature, due to its significance to mountain environmental variations, has been paid increasing attentions in global climate change studies in recent years (Fyfe and Flato 1999; Liu and Chen 2000; Qin et al. 2009).

Several studies have investigated the temperature trend based on the mean surface temperatures in high mountain areas. Some showed the apparent warming trend in their studies. For example, Fyfe and Flato (1999) discovered that the increase of the simulated surface screen temperature is dependent on elevation over the Rocky Mountains in the winter and spring seasons. The warming trend is also observed over the TP regions. Liu and Chen (2000) used a linear regression model to detect the temperature trend over TP and confirmed the warming trend increases with elevation. Oku (2006) analysed the hourly LST geostationary observations over TP from 1996 to 2002 and found an increasing trend. Qin et al. (2009) investigated the recent warming trend in TP with respect to the altitude using monthly MODIS LST data of 2000–2006 and concluded that no increasing trend was observed for elevations higher than 5000 m. Wu et al. (2013) revealed a statistically significant warming in ground surface temperature during 1980–2007 from 16 meteorological stations over central TP region. Zhang et al. (2014) showed that the increasing surface temperature of warming lakes in TP during 2001–2002 was caused by the rise of land and air temperature; meanwhile, the temperature change of cooling lakes, most of which are located at elevations higher than 4200 m, resulted from cold water from the melted glacier. By analysing surface air temperature, Gao, Hao, and Chen (2014) showed a significant warming trend over the TP in the period of 1979–2010.

However, the probability of warming hiatus on global temperature trend is also reported in recent studies. Mears, Schabel, and Wentz (2003) discovered the trend discrepancy between satellites based temperature and *in situ* observations. Fyfe, Gillett, and Zwiers (2013) also found that recent observed global warming trend is significantly less than that of climate models simulation. An et al. (2017) detected a warming hiatus over the TP regions below 4000 m since the late 1990s as well as a delayed warming hiatus higher than 4000 m from mid-2000s. In some studies, even no warming trend is reported (Easterling and Wehner 2009).

Although various studies on the surface temperature trend have been conducted for the last decade, it is still controversial whether it is a warming trend or a warming hiatus over the Earth due to the estimation and integration bias of different data sources. Satellite-derived LST data sets are seldom used in the global climate change studies due to some limitations, e.g. the lack of high-quality long-term climate record (Good et al. 2017), satellite sampling, and impact from the clouds (Jin and Dickinson 1999; Vinnikov et al. 2012). To facilitate the generation of long-term climate record, an original method for the time normalization of LST products was developed (Duan et al. 2014b). Furthermore, many efforts have been made to merge the satellite-derived LST and simulated air temperature based on the relationship between them (Mostovoy et al. 2006; Good 2015; Ouyang et al. 2018). However, the integrated processes and uncertainty of representation of LST would cause unprecedented discrepancies in temperature trend and its variability (Good et al. 2017; Karl et al. 2006).

In this article, for the first time, we independently analysed the Advanced Along-Track Scanning Radiometer (AATSR) LST data set and two temperature outputs (surface skin temperature [TSK] and 2 m air temperature [T2]) from High Asian Refined analysis (HAR)

simulations from 2003 to 2011 in order to get an independent overview of the temperature trend over TP for the last decade.

2. Data and methodology

2.1. Data

The study area of the TP region is between 26°–40° N and 74°–101° E. The TP region is always referred to the region above 3000 m and the average elevation of TP is 4000 m. Figure 1 shows the TP region and the two ground sites of Namco and Qomolangma (Mount Everest) in this study with 30 m spatial resolution digital elevation model from the Shuttle Radar Topography Missions (<http://en.tpdatabase.cn/>; <http://srtm.csi.cgiar.org>).

We conducted the seasonal trend analysis for independent data sources including AATSR LST products, TSK, and 2 m air temperature (T2) data sets simulated from HAR for TP region in 2003–2011 in this study. One kilometre LST, derived from AATSR using the ‘split-window’ method from the AATSR sensors, is one of the most accurate satellite LST data sets produced by GlobTemperature project of European Space Agency Data User Element (Ghent 2012; Good et al. 2017; Ghent et al. 2017) and the absolute biases are 1.00 K in the day and 1.08 K at night (Ghent et al. 2017; Ouyang et al. 2017). HAR TSK and T2 outputs are hourly 10 km gridded data sets dynamically downscaled from the global analysis data using the next-generation mesoscale numerical weather prediction system – Weather Research Forecasting model (MauSSION et al. 2014). HAR provides over 10 years of high-resolution atmospheric data sets including TSK and 2 m air temperature (T2) over TP region. Table 1 gives a general idea of the three data sets.

2.2. Method

The three data sets were validated using a systematic evaluation framework (Ouyang et al. 2018), in which the three data sets are normalized to the same local solar time (AATSR viewing time) and the same spatial resolution (10 km), and a diurnal temperature cycle (DTC) model and an aggregated weighted method are used to avoid the inconsistency among the three data sets and to solve the temporal and spatial mismatch

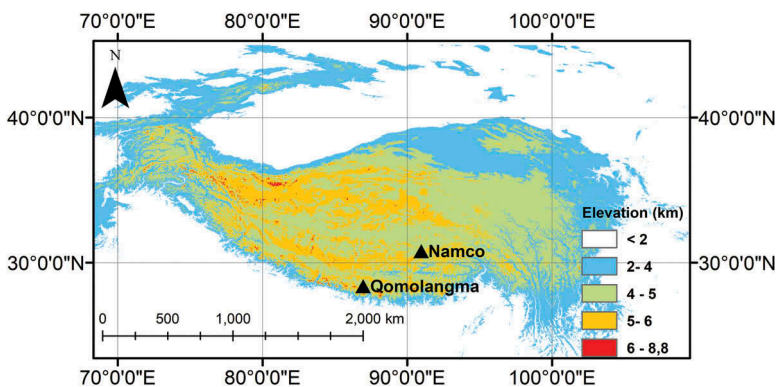


Figure 1. The study area with elevation map as the background over TP region.

Table 1. The temporal and spatial details of the three data sets original information.

Data set name	Temporal resolution	Spatial resolution	Time period	Method	Source
AATSR LST	About twice a day (day and night, around 12 a.m./p.m. Beijing time)	1 km	2002–2012	Split window retrieval	GlobTemperature /ESA DUE
HAR TSK	Hourly	10 km	2001–2014	Downscaling global analysis data	WRF
HAR T2	Hourly	10 km	2001–2014		

problem among the different data sets. We will give an introduction of the two temporal normalization and spatial sampling method in the following two paragraphs.

A DTC model is chosen to time normalize different sources of data sets for temporal normalization (Duan et al. 2013). The DTC model is shown as the following equations,

$$T_1(t) = T_0 + T_a \cos\left(\frac{\pi}{\omega}(t - t_m)\right), \quad t < t_s \quad (1)$$

$$T_2(t) = (T_0 + \delta T) + \left[T_a \cos\left(\frac{\pi}{\omega}(t_s - t_m)\right) - \delta T\right] \frac{k}{(k + t - t_s)}, \quad t \geq t_s \quad (2)$$

where T_1 and T_2 are the temperatures in the separate parts of the model; T_0 is the minimum temperature around sunrise (K); T_a is the temperature amplitude (K); t is the time (hour); ω is the length of daylight hours (hour); t_m is the time of the maximum (hour); t_s is the start of the night-time attenuation (hour); k is the attenuation coefficient; δT is the difference between T_0 and T ($t \rightarrow \infty$). The length of daylight hours (ω) is determined by the sunrise and sunset time. In this article, the sunrise and sunset time value of each pixel was calculated based on the NOAA Solar Calculations (<https://www.esrl.noaa.gov/gmd/grad/solcalc/calcdetails.html>).

A World Geodetic System 1984 (WGS-84) coordinate system with a spatial resolution of 10 km is used to aggregate the cloud-free AATSR data (1 km) to the HAR (10 km) grid for the spatial sampling. The equation is as followed,

$$AGG_m = \frac{\sum_{n=1}^N w_n R_n}{\sum_{n=1}^N w_n} \quad \text{with } w_n = S_{n,m}/S_n \quad (3)$$

where AGG_m is the aggregated LST value of the 10 km pixel, m ; N is the total number of 1 km pixels in the input; w_n is the weight of 1 km cloud-free pixel n ; $S_{n,m}$ is the partial area of pixel n fallen into the target pixel m ; S_n is the total area of pixel n ; and R_n is the temperature value of the pixel n .

The overall correlation coefficients of ground-measured surface temperature and AATSR LST were all above 0.90 over the four ground sites in 2008–2010. In this study, the AATSR overpasses the TP region at around 11:30 a.m./p.m. Beijing Time. The hourly HAR data sets are normalized to the AATSR overpassing time by the DTC model. Meanwhile, the AATSR 1 km data sets are aggregated to 10 km HAR grid by the aggregated weighting method. Note that the AATSR and HAR data sets are all processed to the same spatial resolution at the AATSR overpassing time in order to guarantee that they are compatible during independent comparison. After the data preparation processes of temporal and spatial matching, the commonly used linear regression model (Shrestha et al. 1999; Qin et al. 2009) is used in the trend analysis for easy interpretation

and availability. The trend is also analysed at different elevation ranges. The following equation is used to detect the temperature trend.

$$y = a + bx \quad (4)$$

where y denotes the surface temperature (LST/TSK/T2) (K); x is the time in years; a is the intercept; b is the slope (K year^{-1}) i.e. the warming or cooling rate. A positive slope indicates a warming trend while the negative one refers the cooling trend. The higher the absolute slope, the stronger the warming (or cooling) rate.

We investigate both seasonal trend and spatial variability of LST, TSK, and T2 over TP in 2003–2011 from the day and night data sets. In addition, the temperature trends at two specific sites is analysed to figure out the trend variations in sites surrounded by different land cover with different elevation.

The main processes in this article are based on the linear regression model in Equation. 1. The calculation basis x is 9 years (2003–2011) and each calculation is based on the four different seasons. We conducted independent analysis of temperature trends from four aspects: first, we give an annual seasonal average temperature trend slope on each $10 \times 10 \text{ km}^2$ grid in 2003–2011 to give a spatial–temporal variation of each season in each data set. Second, we consider the study area as a whole and conduct a 9 year regression of its average seasonal temperatures for the whole study area. Third, we choose the grids with elevations higher than 4000 m and calculate the proportion of the grids whose slope is higher than 0 K year^{-1} (warming); we calculate the annual seasonal maximum, minimum, and average temperature trends of the grids, respectively. Finally, we compute the statistics on the average temperature trend of two specific validation sites.

3. Results

3.1. Spatial–temporal temperature trend variation on each grid in the study area

Figure 2 illustrated the spatial variations of regression slopes of spring and winter temperatures from both satellite observations (AATSR LST) and numerical outputs (HAR TSK/T2). To simplify, only the spring and winter seasonal trend variations are listed. For the following sections, we only show the most representative figures to give a general idea of the trend as well. In Figure 2, the trend from AATSR LST is similar to that from HAR TSK/T2 in general. All data sets show that not all grids over TP have the warming trend during 2003–2011, especially in the satellite-derived LST in autumn and winter seasons. Furthermore, a cooling trend (negative) is observed in northeast TP for all the seasons in all the data sets. This finding is inconsistent with those in previous (Duan et al. 2006). Nonetheless, some regions show a distinct warming trend. For example, the Namco area and surroundings (around 30° N , 92.5° E) in the south TP show the warming trend for all the seasons in all the data sets. It should be mentioned that due to the heavily impact of cloud effect on the satellite-derived LST retrieval, the temperature trend of spring night shown in the northwest (Figure 2 (c)(i)) was skewed and abnormal; the cloud effect would also affect the trends of the HAR data sets since they are sampled corresponding to the AATSR tracks.

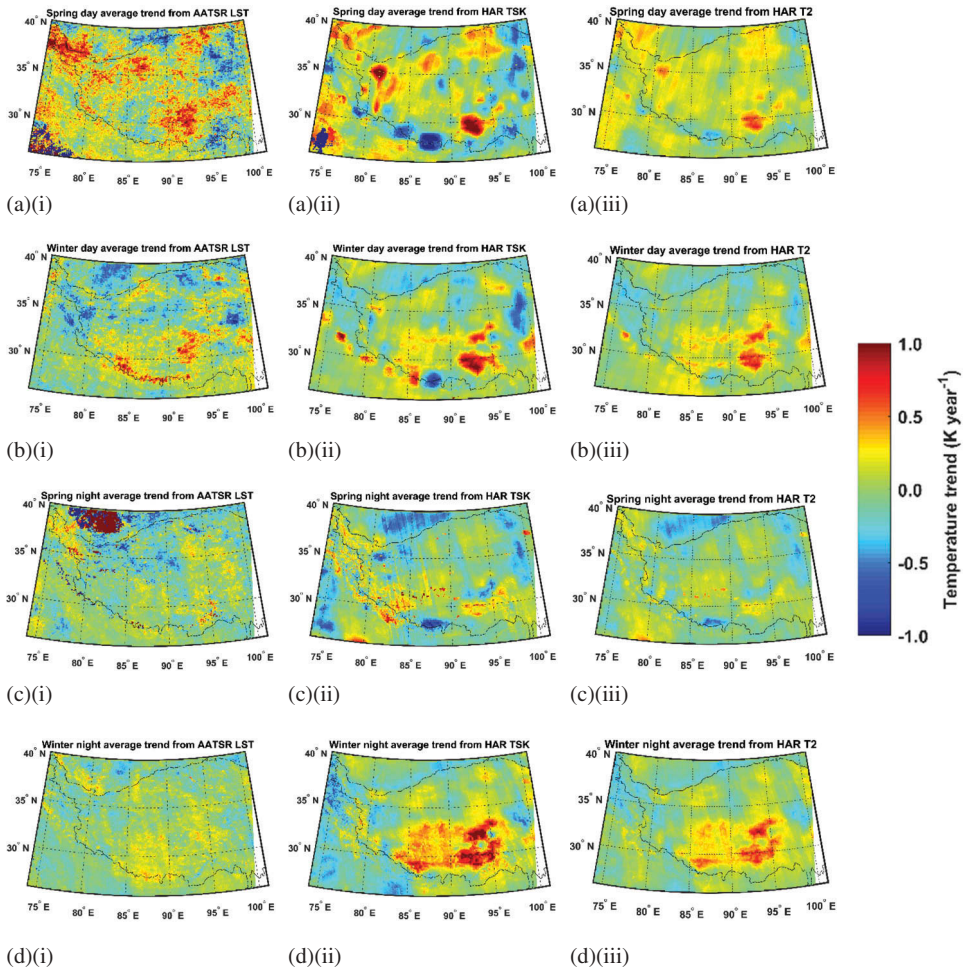


Figure 2. The spatial seasonal variations of temperature trends (slope, b) from AATSR LST and HAR TSK/T2 over the entire TP region during 2003–2011. Spring day average trends are shown in (a)(i) AATSR LST, (a)(ii) HAR TSK, (a)(iii) HAR T2; winter day average trends are shown in (b)(i) AATSR LST, (b)(ii) HAR TSK, (b)(iii) HAR T2; spring night average trends are shown in (c)(i) AATSR LST, (c)(ii) HAR TSK, (c)(iii) HAR T2; winter night average trends are shown in (d)(i) AATSR LST, (d)(ii) HAR TSK, (d)(iii) HAR T2.

Warming trends from TSK and T2 are stronger than their corresponding trends from LST in all seasons except summer. Similar result is also found by Jin, Dickinson, and Vogelmann (1997) in the low- and mid-latitude regions and Fyfe, Gillett, and Zwiers (2013) in global mean surface temperature analysis. The night temperature shows a distinct faster warming trend than day ones in HAR TSK and T2 outputs (Duan and Xiao 2015), whereas this result cannot be concluded from AATSR observations.

3.2. The averaged trend of the whole study area

Further studies are also conducted on the trend of total average temperature over the whole TP region at both day and night during last decade (Figure 3). The average day

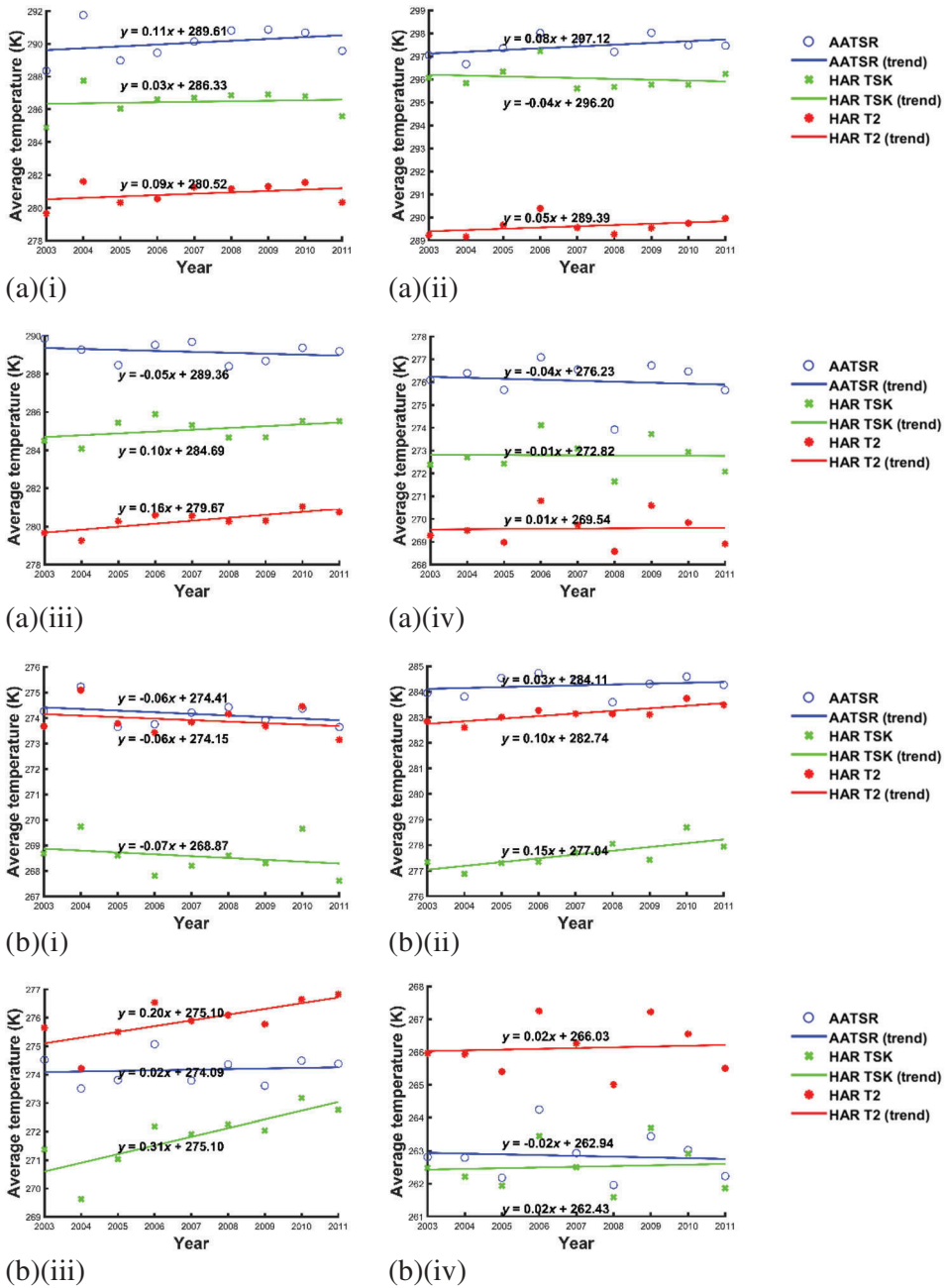


Figure 3. The average temperatures and their trends over TP region during 2003–2011. The trends are presented by the slope calculated from the linear regression method through the nine year. Day: (a)(i) spring, (a)(ii) summer, (a)(iii) autumn, (a)(iv) winter; night: (b)(i) spring, (b)(ii) summer, (b)(iii) autumn, (b)(iv) winter.

AATSR LST is higher than corresponding HAR TSK and T2. The night air temperature from HAR T2 in autumn and winter is higher than the corresponding AATSR LST over TP from 2003 to 2011. This is usually caused by the lower solar insolation at night (Good 2016).

The overall slope of the day temperature warming trend from all the data sets is 0.04 K year^{-1} , while that of the night warming trend is 0.05 K year^{-1} . In each data set, the day warming trend slopes from AATSR LST, HAR TSK, and HAR T2 are 0.04, 0.04, and 0.08 K year^{-1} , respectively. The night warming trend slopes of the corresponding data sets are 0.05, 0.01, and 0.1 K year^{-1} , respectively. The night air temperature from HAR T2 shows a more distinct warming trend than the other two data sets.

During spring night, the trend slope from both AATSR LST and HAR T2 is 0.06 K year^{-1} and the average temperature values are 274.41 and 274.15 K for the whole region, respectively. The exception occurred at autumn night: AATSR LST shows no obvious warming trend ($b = 0.02 \text{ K year}^{-1}$), whereas both HAR TSK and T2 show warming trend of 0.20 and 0.31 K year^{-1} , respectively. These results match those in Section 3.1, where the warming trend is distinct from HAR data sets, especially in HAR TSK. Except this inconsistent, the trends in all AATSR LST and HAR TSK/T2 show the similar results: the warming trend is not obvious, where the average (calculated from 15 positive values only) and largest slope b value are 0.10 and 0.31 K year^{-1} , respectively. Both AATSR and HAR data sets even show the negative slope value (cooling trend) during spring night. In consideration of the unprecedented extreme climate events, cloud contamination, satellite noise, and simulation bias in the computation, the frequency is not distinct at all.

3.3. Temperature trend of areas with elevation above 4000 m

Temperature trends in the area above 4000 m are analysed and the result is shown in Figure 4. The results show that in these areas, the proportion of areas with the slope higher than 0 K year^{-1} (warming trend) is less than 50% except for the autumn day from HAR data sets. The HAR data sets show a more distinct warming trend than the AATSR observations, especially for the HAR T2 data sets. The proportions of the area with the warming trend from HAR T2 data sets are higher than that from AATSR LST and HAR TSK for almost all seasons except winter night. It means the increase of air temperature is more distinct than that of surface temperature over TP region during the last decade. The discrepancies between AATSR LST and HAR T2 in autumn are higher than that in the other three seasons. The smallest discrepancy among the three data sets is observed in winter.

In addition, the frequency of areas with the warming trend at night is higher than that in the day by nearly 10%. The results are consistent with the previous studies that the warming is caused mainly by the increase in minimum temperature and the night warming is stronger (Duan et al. 2006; Zhai and Pan 2003). However, different from a previous study (Duan et al. 2006), the winter warming is not stronger than other seasons during the study period.

The summer day HAR TSK average warming trend has the lowest frequency among the three data sets, where the frequency of warming from AATSR TSK and HAR T2 is almost two times of that from HAR TSK. This result is consistent with the spatial trend variations in Section 3.1.

3.4. Temperature trends of two ground sites

We have chosen two ground sites (Namco and Qomolangma) with different surrounding land surface type and elevation to analyse their temperature trends, including the

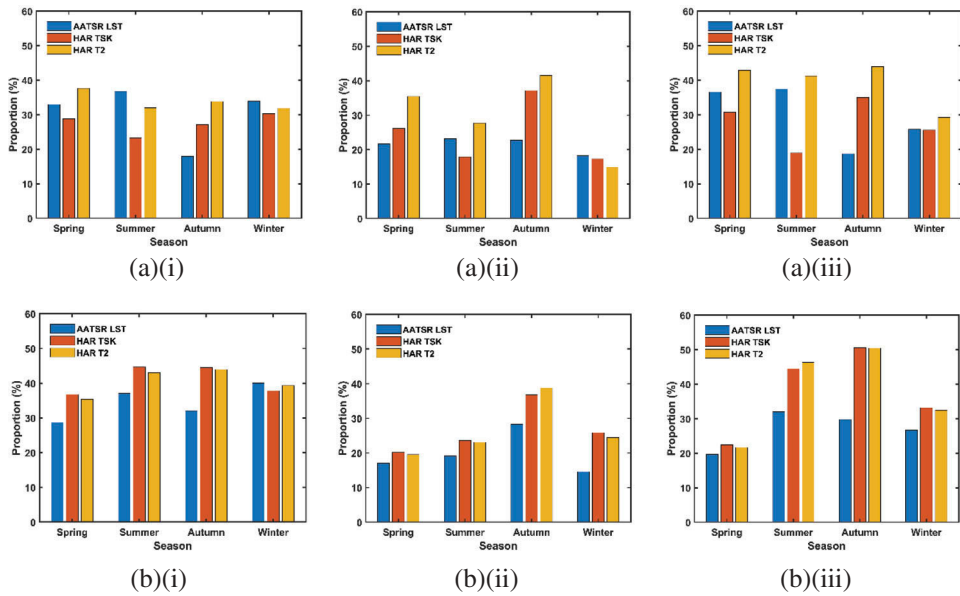


Figure 4. The proportion of areas with elevation over 4000 m that have a positive slope (warming trend) during 2003–2011. Day: (a)(i) maximum temperature, (a)(ii) minimum temperature, (a)(iii) average temperature. Night: (b)(i) maximum temperature, (b)(ii) minimum temperature, (b)(iii) average temperature.

annual maximum, minimum, and average temperatures at both day and night. Namco site with elevation of 4730 m is located around the near lake alpine steppe land surface type, while Qomolangma with elevation of 4293 m is surrounded by the riverbed gravel land surface type. The Namco site shows a clear warming trend at both day and night from the AATSR observations and HAR outputs (Figure 5). This result is consistent with those from Section 3.1. During spring and summer, the pattern of day and night of all data sets are similar. The discrepancy is that the trend observed from AATSR LST shows a slight cooling (-0.1 K year^{-1}) trend during the autumn night, whereas the faster warming trend (0.5 K year^{-1}) is observed from AATSR during winter day.

In contrast, the results at Qomolangma site show a distinct cooling trend, especially from the day temperature of HAR outputs. For AATSR LST observations, the cooling trend is detected in the day temperature and a slight warming trend is observed in the night temperature. The day HAR TSK shows a cooling trend with the slope below -0.5 K year^{-1} in spring, summer, and autumn. In general, although the trends of autumn and winter night are not apparent, the Qomolangma site has demonstrated a cooling trend during last decade from HAR outputs. The trends, both warming one in Namco site and cooling one in Qomolangma site, from AATSR LST are weaker than those from HAR outputs.

3.5. Discussion

Many efforts have been paid in the climate change study of TP region through both simulated weather data and ground observations. The satellite-derived LST observations

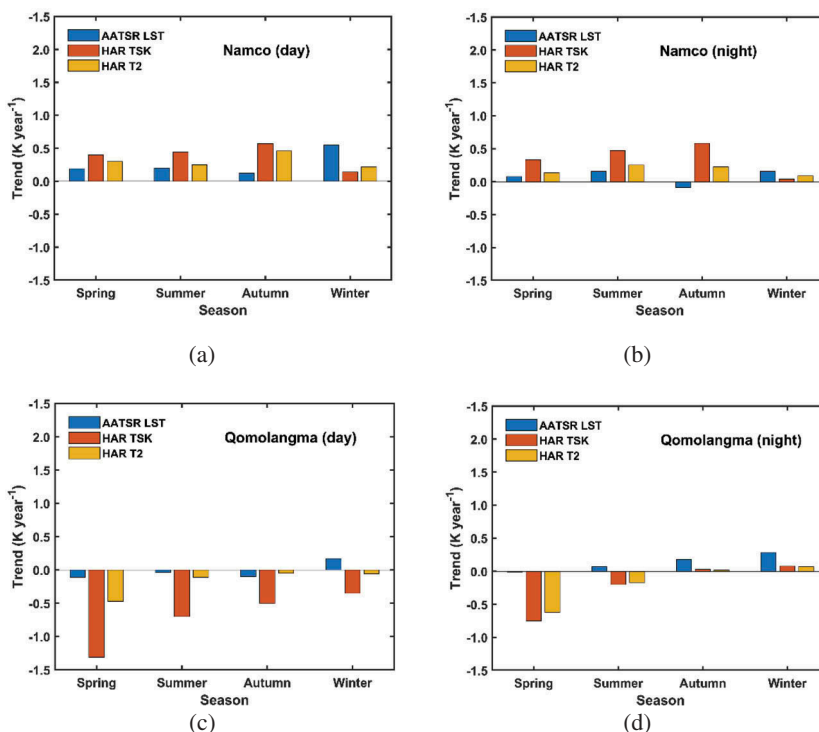


Figure 5. Two trend slopes from different data sets for two ground sites during 2003–2011. Day average trends are shown in (a) Namco, (c) Qomolangma; night average trends are shown in (b) Namco, (d) Qomolangma.

are often considered to be difficult to be used in the climate change studies due to their limited time span, cloud problems, and other inherent retrieval problems. The major problem is, as Good et al. 2017 mentioned, that the satellite observation only gives a ‘snapshot’ of the ground surface, limiting the study of the whole day overall status. The short span of AATSR satellite observations is one limitation in this article. As Hua et al. (2017) mentioned that the uncertainties decrease steadily with time by using meteorological station observations. It is logical when it comes to the satellite observations. Therefore, the best way to decrease the uncertainty is to prolong the observation span.

Despite these limitations, satellite observations can provide wide spatial coverage and high resolutions over the sparsely populated TP region (Jin and Mullens 2012). This work gives a preliminary study on the independent analysis based on satellite observations and simulated data in order to avoid the error caused by the integration processes (Karl et al. 2006). Moreover, the comparison among the three data sets helps to qualitatively and quantitatively understand the trend clearly and independently. It also gave a comparison between different data sets over the same conditions.

This work follows the previous studies and gives the similar results as former studies. The first consistency is that the simulation warming trends are higher than the satellite observations (Jin, Dickinson, and Vogelmann 1997; Fyfe, Gillett, and Zwiers 2013) for almost all the conditions over the study period. Second, the frequencies of maximum warming trends are lower than either the average or the minimum trends in all the data

sets. This is consistent with the former studies that the daily minimum has risen faster than the daily maximum and a narrowing diurnal range of LST (Oku et al. 2006). Third, the Qomolangma site (4293 m) shows a distinct cooling trend, which is consistent with the study of Qin et al. (2009) that a slight decline near the highest elevations is detected.

However, some discrepancies from previous studies are also demonstrated in our work. First, the overall warming trend is not distinct over the TP region except the Namco surroundings over the last decade. Second, the cooling trend is detected in northeast TP for all seasons from all data sets which is inconsistent with the previous studies that the air temperature is warming in the middle and east TP region (Duan et al. 2006). Third, the winter warming is not as distinct as the former studies (Duan and Xiao 2015; Hua et al. 2017). Fourth, the warming trend is not distinct over area higher than 4000 m (Qin et al. 2009) either.

4. Conclusion

This study uses independent and simultaneous satellite observations and numerical data sets for the first time to analyse the spatial and temporal temperature trend over TP for the last decade. We analysed the seasonal and spatial TP region temperature trend independently, as well as the characteristics of areas higher than 4000 m.

In our study, the overall trend slope for the day from all the data sets is 0.04 K year^{-1} , while the night trend slope is 0.05 K year^{-1} . For each data set, the day trend slopes for AATSR LST, HAR TSK and HAR T2 are 0.04, 0.04, and 0.08 K year^{-1} , respectively. The night trend slopes for corresponding data set are 0.05, 0.01, and 0.1 K year^{-1} , respectively. The night air temperature from HAR T2 (0.08 and 0.1 K year^{-1} during day and night, respectively) shows a more distinct warming trend than the other two data sets. The results from the area with elevation higher than 4000 m show that in these areas, the frequency of warming rate is less than 50% except for the autumn day from HAR data sets. The Namco and Qomolangma sites show an apparent different trend of warming and cooling trend, respectively.

The consistent results from both satellite observations and numerical outputs show that (1) the warming trend over the entire TP is not distinct during last decade, especially in northeast TP. (2) The spring day average AATSR LST trend is consistent with the HAR TSK and T2 trend. (3) The temperature of the region around Namco is actually increasing during last decade in all seasons from all data sets. (4) The results at site Qomolangma show a distinct cooling trend, especially in day temperatures.

Meanwhile, the discrepancy among the different data sets shows that the warming trend from simulation outputs is higher than that from the AATSR observations, especially in autumn and winter. Moreover, the increase of air temperature is more distinct than that of surface temperature over TP for the last decade. This article gives a possibility of using satellite-based LST data and simulated temperature data together in the regional and global climate analysis.

The limitation of the studies also includes two parts: first, the clear-sky satellite observations sampling without cloudy-sky temperature information might mask the true LST trends (Wang and Key, 2003; Westermann et al., 2012); second, the 9 year trend comparison may not be enough for the climatic change studies. In the future

studies, we will focus on the long-term temperature analysis from different sources of data sets under all sky conditions.

The urgent need for the inclusion of long-term remote-sensing-based LST data in the global change studies has been mentioned in the Intergovernmental Panel on Climate Change (Oku et al. 2006). This work provides a clear picture of climate change patterns through satellite-derived LST data.

Acknowledgements

The authors would like to thank the European Space Agency (ESA) Data User Element (DUE) GlobTemperature Project for providing the AATSR GlobTemperature Level-2/Level-3 v1.0 LST data. The authors would also like to thank the Chair of Climatology, TU Berlin for the HAR data set. Xiaoying Ouyang thanks China Scholarship Council for her stay in Queen's University, Canada.

Disclosure statement

No potential conflict of interest was reported by the authors.

Funding

This research is supported by the National Natural Science Foundation of China (NSFC) [Grant Numbers 41571366 and 41101326] and Canada National Science and Engineering Research Council (NSERC) Discovery Grant.

ORCID

Xiaoying Ouyang  <http://orcid.org/0000-0002-4454-4101>

Dongmei Chen  <http://orcid.org/0000-0001-5419-8735>

References

- An, W., S. Hou, Y. Hu, and S. Wu. 2017. "Delayed Warming Hiatus over the Tibetan Plateau." *Earth and Space Science* 4 (3): 128–137. doi:10.1002/2016EA000179.
- Cheng, J., S. Liang, J. Wang, and X. Li. 2010. "A Stepwise Refining Algorithm of Temperature and Emissivity Separation for Hyperspectral Thermal Infrared Data." *IEEE Transactions on Geoscience and Remote Sensing* 48 (3): 1588–1597. doi:10.1109/TGRS.2009.2029852.
- Duan, A., G. Wu, Q. Zhang, and Y. Liu. 2006. "New Proofs of the Recent Climate Warming over the Tibetan Plateau as a Result of the Increasing Greenhouse Gases Emissions." *Chinese Science Bulletin* 51 (11): 1396–1400. doi:10.1007/s11434-006-1396-6.
- Duan, A., and Z. Xiao. 2015. "Does the Climate Warming Hiatus Exist over the Tibetan Plateau?" *Scientific Reports* 5. doi:10.1038/srep13711.
- Duan, S.-B., Z.-L. Li, B.-H. Tang, H. Wu, and R. Tang. 2014a. "Direct Estimation of Land-Surface Diurnal Temperature Cycle Model Parameters from MSG–SEVIRI Brightness Temperatures under Clear Sky Conditions." *Remote Sensing of Environment* 150: 34–43. doi:10.1016/j.rse.2014.04.017.
- Duan, S.-B., Z.-L. Li, B.-H. Tang, H. Wu, and R. Tang. 2014b. "Generation of a Time-Consistent Land Surface Temperature Product from MODIS Data." *Remote Sensing of Environment* 140: 339–349. doi:10.1016/j.rse.2013.09.003.

- Duan, S.-B., Z.-L. Li, H. Wu, B.-H. Tang, X. Jiang, and G. Zhou. 2013. "Modeling of Day-To-Day Temporal Progression of Clear-Sky Land Surface Temperature." *IEEE Geoscience and Remote Sensing Letters* 10 (5): 1050–1054. doi:10.1109/LGRS.2012.2228465.
- Duan, S.-B., Z.-L. Li, and P. Leng. 2017. "A Framework for the Retrieval of All-Weather Land Surface Temperature at a High Spatial Resolution from Polar-Orbiting Thermal Infrared and Passive Microwave Data." *Remote Sensing of Environment* 195: 107–117. doi:10.1016/j.rse.2017.04.008.
- Easterling, D. R., and M. F. Wehner. 2009. "Is the Climate Warming or Cooling?" *Geophysical Research Letters* 36: 8. doi:10.1029/2009GL037810.
- Fyfe, J. C., and G. M. Flato. 1999. "Enhanced Climate Change and Its Detection over the Rocky Mountains." *Journal of Climate* 12 (1): 230–243. doi:10.1175/1520-0442-12.1.230.
- Fyfe, J. C., N. P. Gillett, and F. W. Zwiers. 2013. "Overestimated Global Warming over the past 20 Years." *Nature Climate Change* 3 (9): 767–769. doi:10.1038/nclimate1972.
- Gao, L., L. Hao, and X. W. Chen. 2014. "Evaluation of ERA-interim Monthly Temperature Data over the Tibetan Plateau." *Journal of Mountain Science* 11 (5): 1154–1168. doi:10.1007/s11629-014-3013-5. doi:10.1007/s11629-014-3013-5.
- Ghent, D. 2012. "Land Surface Temperature Validation and Algorithm Verification." Report to European Space Agency:1–17.
- Ghent, D., G. Corlett, F. M. Göttsche, and J. Remedios. 2017. "Global Land Surface Temperature from the Along-Track Scanning Radiometers." *Journal of Geophysical Research: Atmospheres* 122: 22.
- Good, E. 2015. "Daily Minimum and Maximum Surface Air Temperatures from Geostationary Satellite Data." *Journal of Geophysical Research: Atmospheres* 120 (6): 2306–2324.
- Good, E. J. 2016. "An in Situ-Based Analysis of the Relationship between Land Surface "Skin" and Screen-Level Air Temperatures." *Journal of Geophysical Research: Atmospheres* 121 (15): 8801–8819.
- Good, E. J., D. J. Ghent, C. E. Bulgin, and J. J. Remedios. 2017. "A Spatio-Temporal Analysis of the Relationship between Near-Surface Air Temperature and Satellite Land Surface Temperatures Using 17 Years of Data from the ATSR Series." *Journal of Geophysical Research: Atmospheres* 122: 9185–9210. doi: 10.1002/2017JD026880.
- Hua, W., G. Fan, Y. Zhang, L. Zhu, X. Wen, Y. Zhang, X. Lai, B. Wang, M. Zhang, and Y. Hu. 2017. "Trends and Uncertainties in Surface Air Temperature over the Tibetan Plateau, 1951–2013." *Journal of Meteorological Research* 31 (2): 420–430. doi:10.1007/s13351-017-6013-x.
- Jin, M., R. Dickinson, and A. Vogelmann. 1997. "A Comparison of CCM2–BATS Skin Temperature and Surface-Air Temperature with Satellite and Surface Observations." *Journal of Climate* 10 (7): 1505–1524. doi:10.1175/1520-0442(1997)010<1505:ACOCBS>2.0.CO;2.
- Jin, M. L., and R. E. Dickinson. 1999. "Interpolation of Surface Radiative Temperature Measured from Polar Orbiting Satellites to a Diurnal Cycle - 1. Without Clouds." *Journal of Geophysical Research-Atmospheres* 104 (D2): 2105–2116. doi:10.1029/1998jd200005. doi:10.1029/1998jd200005.
- Jin, M. S., and T. J. Mullens. 2012. "Land-Biosphere-Atmosphere Interactions over the Tibetan Plateau from MODIS Observations." *Environmental Research Letters* 7: 1. doi:10.1088/1748-9326/7/1/014003. doi:10.1088/1748-9326/7/1/014003.
- Karl, T. R., S. J. Hassol, C. D. Miller, and W. L. Murray. 2006. *Temperature Trends in the Lower Atmosphere. Steps for Understanding and Reconciling Differences*. MD: National Oceanic and Atmospheric Administration
- Li, Z. L., B. H. Tang, H. Wu, H. Z. Ren, G. J. Yan, Z. M. Wan, I. F. Trigo, and J. A. Sobrino. 2013. "Satellite-Derived Land Surface Temperature: Current Status and Perspectives." *Remote Sensing of Environment* 131: 14–37. doi:10.1016/j.rse.2012.12.008. doi:10.1016/j.rse.2012.12.008.
- Liu, X. D., and B. D. Chen. 2000. "Climatic Warming in the Tibetan Plateau during Recent Decades." *International Journal of Climatology* 20 (14): 1729–1742. doi:10.1002/1097-0088(20001130)20:14<1729::aid-joc556>3.0.co;2-y. doi:10.1002/1097-0088(20001130)20:14<1729::aid-joc556>3.0.co;2-y.
- Maussion, F., D. Scherer, T. Molg, E. Collier, J. Curio, and R. Finkelburg. 2014. "Precipitation Seasonality and Variability over the Tibetan Plateau as Resolved by the High Asia Reanalysis." *Journal of Climate* 27 (5): 1910–1927. doi:10.1175/jcli-d-13-00282.1. doi:10.1175/jcli-d-13-00282.1.
- Mears, C. A., M. C. Schabel, and F. J. Wentz. 2003. "A Reanalysis of the MSU Channel 2 Tropospheric Temperature Record." *Journal of Climate* 16 (22): 3650–3664. doi:10.1175/1520-0442(2003)016<3650:AROTMC>2.0.CO;2.

- Mostovoy, G. V., R. L. King, K. R. Reddy, V. G. Kakani, and M. G. Filippova. 2006. "Statistical Estimation of Daily Maximum and Minimum Air Temperatures from MODIS LST Data over the State of Mississippi." *GIScience & Remote Sensing* 43 (1): 78–110. doi:[10.2747/1548-1603.43.1.78](https://doi.org/10.2747/1548-1603.43.1.78).
- Oku, Y., H. Ishikawa, S. Haginoya, and Y. Ma. 2006. "Recent Trends in Land Surface Temperature on the Tibetan Plateau." *Journal of Climate* 19 (12): 2995–3003. doi:[10.1175/JCLI3811.1](https://doi.org/10.1175/JCLI3811.1).
- Ouyang, X., D. Chen, S.-B. Duan, Y. Lei, Y. Dou, and G. Hu. 2017. "Validation and Analysis of Long-Term AATSR Land Surface Temperature Product in the Heihe River Basin, China." *Remote Sensing* 9 (2): 152. doi:[10.3390/rs9020152](https://doi.org/10.3390/rs9020152).
- Ouyang, X., D. Chen, and Y. Lei. 2018. "A Generalized Evaluation Scheme for Comparing Temperature Products from Satellite Observations, Numerical Weather Model, and Ground Measurements over the Tibetan Plateau." *IEEE Transactions on Geoscience and Remote Sensing*. doi: [10.1109/TGRS.2018.2815272](https://doi.org/10.1109/TGRS.2018.2815272).
- Qin, J., K. Yang, S. L. Liang, and X. F. Guo. 2009. "The Altitudinal Dependence of Recent Rapid Warming over the Tibetan Plateau." *Climatic Change* 97 (1–2): 321–327. doi:[10.1007/s10584-009-9733-9](https://doi.org/10.1007/s10584-009-9733-9).
- Qin, Z., G. Dall'Olmo, A. Karnieli, and P. Berliner. 2001a. "Derivation of Split Window Algorithm and Its Sensitivity Analysis for Retrieving Land Surface Temperature from NOAA-advanced Very High Resolution Radiometer Data." *Journal of Geophysical Research: Atmospheres* 106 (D19): 22655–22670. doi:[10.1029/2000JD900452](https://doi.org/10.1029/2000JD900452).
- Qin, Z., A. Karnieli, and P. Berliner. 2001b. "A Mono-Window Algorithm for Retrieving Land Surface Temperature from Landsat TM Data and Its Application to the Israel-Egypt Border Region." *International Journal of Remote Sensing* 22 (18): 3719–3746. doi:[10.1080/01431160010006971](https://doi.org/10.1080/01431160010006971).
- Shrestha, A. B., C. P. Wake, P. A. Mayewski, and J. E. Dibb. 1999. "Maximum Temperature Trends in the Himalaya and Its Vicinity: An Analysis Based on Temperature Records from Nepal for the Period 1971–94." *Journal of Climate* 12 (9): 2775–2786. doi:[10.1175/1520-0442\(1999\)012<2775:MTTITH>2.0.CO;2](https://doi.org/10.1175/1520-0442(1999)012<2775:MTTITH>2.0.CO;2).
- Vinnikov, K. Y., Y. Y. Yu, M. D. Goldberg, D. Tarpley, P. Romanov, I. Laszlo, and M. Chen. 2012. "Angular Anisotropy of Satellite Observations of Land Surface Temperature." *Geophysical Research Letters* 39. doi:[10.1029/2012gl054059](https://doi.org/10.1029/2012gl054059).
- Wang, X., and J.R. Key. 2003. "Recent Trends in Arctic Surface, Cloud, and Radiation Properties from Space." *Science* 299 (5613): 1725–1728. doi:[10.1126/science.1078065](https://doi.org/10.1126/science.1078065).
- Westermann, S., M. Langer, and B. Julia. 2012. "Systematic Bias of Average Winter-Time Land Surface Temperatures Inferred from MODIS at a Site on Svalbard, Norway." *Remote Sensing Of Environment* 118 (2012): 162–167. doi:[10.1016/j.rse.2011.10.025](https://doi.org/10.1016/j.rse.2011.10.025).
- Wu, T., L. Zhao, R. Li, Q. Wang, C. Xie, and Q. Pang. 2013. "Recent Ground Surface Warming and Its Effects on Permafrost on the Central Qinghai-Tibet Plateau." *International Journal of Climatology* 33 (4): 920–930. doi:[10.1002/joc.v33.4](https://doi.org/10.1002/joc.v33.4).
- Zhai, P., and X. Pan. 2003. "Trends in Temperature Extremes during 1951–1999 in China." *Geophysical Research Letters* 30: 17. doi:[10.1029/2003GL018004](https://doi.org/10.1029/2003GL018004).
- Zhang, G. Q., T. D. Yao, H. J. Xie, J. Qin, Q. H. Ye, Y. F. Dai, and R. F. Guo. 2014. "Estimating Surface Temperature Changes of Lakes in the Tibetan Plateau Using MODIS LST Data." *Journal of Geophysical Research-Atmospheres* 119 (14): 8552–8567. doi:[10.1002/2014jd021615](https://doi.org/10.1002/2014jd021615).